J Mater Sci: Mater Med (2011) 22:1293–1302
DOI 10.1007/s10856-011-4301-z

Study of the in vitro corrosion behavior and biocompatibility of Zr-2.5Nb and Zr-1.5Nb-1Ta (at%) crystalline alloys

F. Rosalbino · D. Macciò · P. Giannoni · R. Quarto · A. Saccone

Received: 25 October 2010 / Accepted: 18 March 2011 / Published online: 2 April 2011

Abstract The in vitro corrosion behavior and biocompatibility of two Zr alloys, Zr-2.5Nb, employed for the manufacture of CANDU reactor pressure tubes, and Zr-1.5Nb-1Ta (at%), for use as implant materials have been assessed and compared with those of Grade 2 Ti, which is known to be a highly compatible metallic biomaterial. The in vitro corrosion resistance was investigated by open circuit potential and electrochemical impedance spectroscopy (EIS) measurements, as a function of exposure time to an artificial physiological environment (Ringer's solution). Open circuit potential values indicated that both the Zr alloys and Grade 2 Ti undergo spontaneous passivation due to spontaneously formed oxide film passivating the metallic surface, in the aggressive environment. It also indicated that the tendency for the formation of a spontaneous oxide is greater for the Zr-1.5Nb-1Ta alloy and that this oxide has better corrosion protection characteristics than the ones formed on Grade 2 Ti or on the Zr-2.5Nb alloy. EIS study showed high impedance values for all samples, increasing with exposure time, indicating an improvement in corrosion resistance of the spontaneous oxide film. The fit obtained suggests a single passive film presents on the metals surface, improving their resistance with exposure time, presenting the highest values to the Zr-1.5Nb-1Ta alloy. For the biocompatibility analysis human osteosarcoma cell line (Saos-2) and human primary bone marrow stromal cells (BMSC) were used. Biocompatibility tests showed that Saos-2 cells grow rapidly, independently of the surface, due to reduced dependency from matrix deposition and microenvironment recognition. BMSC instead display a reduced proliferation, possibly caused by a reduced crosstalk with the metal surface microenvironment. However, once the substrate has been colonized, BMSC seem to respond properly to osteoinduction stimuli, thus supporting a substantial equivalence in the biocompatibility among the Zr alloys and Grade 2 titanium. In summary, high in vitro corrosion resistance together with satisfactory biocompatibility make the Zr-2.5Nb and Zr-1.5Nb-1Ta crystalline alloys promising biomaterials for surgical implants.

F. Rosalbino (✉)
Dipartimento di Scienza dei Materiali e Ingegneria Chimica, Politecnico di Torino, Corso Duca degli Abruzzi, 24, 10129 Turin, Italy
e-mail: francesco.rosalbino@polito.it

D. Macciò · A. Saccone
Dipartimento di Chimica e Chimica Industriale, Università degli Studi di Genova, Via Dodecaneso, 31, 16146 Genoa, Italy

P. Giannoni
Laboratorio di Cellule Staminali, Centro Biotecnologie Avanzate, Largo R. Benzi, 10, 16132 Genoa, Italy

R. Quarto
Dipartimento di Medicina Sperimentale, DIMES Università degli Studi di Genova, Viale Benedetto XV, 8, 16132 Genoa, Italy

1 Introduction

Zr, Nb and Ta belong to a group of elements (along with Al, Ti, W) known as valve-metals, which are usually covered by a spontaneously formed thin oxide layer; this constitutes a barrier between the metal and the environment. Typical values for the initial thickness of these oxide layers formed in air at room temperature are in the range 2–5 nm, though this thickness can be greatly increased by anodic oxidation [1]. These oxides, which can be electric insulators or semiconductors and resistant to attack by most mineral acids, organic and alkaline solutions [2], have been

the subject of intense investigations concerning their stability and physical properties [3–7].

Because of the high corrosion resistance of valve metals in media of an oxidizing nature or containing chloride ions, the areas of application of these metals and their alloys were extended to biomedical uses, since most body fluids in the human organism contain chloride ions [10]; thus, rapid progress has occurred in the areas of medical instrumentation and surgical implants [11].

Nowadays, as the fraction of senior citizens in the population of most countries is increasing, the demand of artificial implants has been growing, thus requiring more investigations on materials for this purpose [12–14]. In order to expand the use of alloys as biomaterials, the development and study of new alloys presenting excellent biocompatibility and sufficient mechanical/corrosion resistance are necessary. Many studies have shown that materials of low elasticity modulus (more flexible) can better simulate a natural femur. Hence, there is an interest in alloys of such characteristics in order to obtain a new generation of materials for implants. In this context, the study of zirconium alloys has become attractive due to chemical properties similar to those of titanium alloys. Conventional Zr metal shows acceptable mechanical strength and good biocompatibility, thereby it is a material of interest for surgical implants [15, 16]. In vivo evidences have indicated that zirconium implants exhibit good osteointegration [17, 18] and studies comparing zirconium and titanium implants showed that the degree of bone-implant contact is higher in the case of zirconium [19, 20].

There are several Zr alloys utilized in the nuclear industry that could be considered for medical applications including the alloys Zircaloy-2, Zircaloy-4, Zr-1Nb and Zr-2.5Nb. The Zr-1Nb alloy is being used as an advanced cladding material for French pressurized water reactors, under the designation M5, and for similar application in Russian reactors under the designation E110. The Zr-2.5Nb alloy has been used extensively for the manufacture of Canadian Deuterium Uranium (CANDU) reactor pressure tubes [21]. Niobium imparts creep resistance and additional elevated temperature strength. Niobium, in and of itself, is highly corrosion resistant, in addition to being a strengthener to zirconium. Tantalum is more corrosion resistant than niobium due to the higher stability of its oxide. The superior corrosion resistance and biocompatibility of tantalum have been extensively evaluated and recognized by several researchers [22–24]. However, tantalum exhibits only a limited mechanical resistance [25]. Thus, considering the individual characteristics of niobium and tantalum, Zr–Nb–Ta ternary alloys are expected to present a good combination of mechanical resistance, corrosion resistance and biocompatibility.

Very few works are available on the in vitro corrosion behavior of Zr alloys in simulated biological solutions and their in vitro biocompatibility has scarcely been explored [26]. Niobium and tantalum alloying additions appear to improve the corrosion resistance of zirconium in simulated physiologic media, but the electrochemical data are very limited [27].

Aim of the present work was to study the in vitro corrosion resistance and biocompatibility of two Zr alloys, Zr-2.5Nb and Zr-1.5Nb-1Ta (at%), from here onward also identified with the terms BIN (binary alloy) and TER (ternary alloy) respectively, formed from nontoxic elements [12, 28, 29], for use as implant materials. The in vitro corrosion behavior of the two alloys was assessed in an artificial physiological solution using open circuit potential and electrochemical impedance spectroscopy (EIS) measurements. For comparison purposes, commercially pure Grade 2 titanium, which is known to be a highly compatible metallic biomaterial, was also investigated.

2 Experimental

2.1 Samples preparation and phase analysis techniques

The metals used were Zr (99.8 mass%, NewMet Koch, Waltham Abbey, UK), Nb and Ta (99.6 mass%, H.C.Starck, Inc., 45 Industrial place, Newton, MA 02461–1951/USA), Ti grade 2 (L. Klein SA, Chemin du Long-Champ 110, Case postale 973 CH-2501 Biel—Switzerland).

The Zr-2.5Nb and Zr-1.5Nb-1Ta (at.%) crystalline alloys, with a mass of about 2 g each, were prepared by arc melting from starting metals in pieces, in inert Ar atmosphere, after some washing under vacuum. The samples were melt and reversed at least 5 times to assure homogeneity, and let cooling in Ar till room temperature.

Before electrochemical measurements, phase analysis of all the samples was carried out so as to check overall composition, and morphology. Moreover, crystal structure of the phases was verified. Metallographic and X-ray diffraction (XRD) analyses were used. The first was performed on the samples, dry-polished using standard methods, by electron microscopy. The instrument was a Zeiss scanning electron microscope (SEM), model EVO 40, working at a 20 kV acceleration, equipped with the SmartSEM^{TM} software. Quantitative electron probe microanalysis (EPMA) of the phases was carried out using an energy dispersive X-ray electron probe analyser (Tetralink Pentafet model, Oxford Instruments). XRD analysis was used in order to identify the crystal structures of the phases, and to determine lattice parameters. The measurements were performed on powdered samples mounted

on a zero background Si support, by means of a vertical diffractometer (Philip X'Pert model). Operating conditions and data handling for these techniques are thoroughly described elsewhere [30].

Proofs for biocompatibility tests were made as follows. Samples for in vitro measurements were prepared cutting in thin slices the Grade 2 titanium and the tested Zr alloys, by means of a precision cut-off machine Struers Secotom 10, equipped by an abrasive precision cut-off wheel (HV 500–800). Small discs, 4 mm diameter and 1–1.5 mm thickness, were obtained. For each metal, Grade 2 Ti, Zr-2.5Nb and Zr-1.5Nb-1Ta alloys, a total of 24 discs was used. The surfaces were lead to the same roughness by dry polishing with extra fine emery paper (320 grit size). All the samples were finally washed in an ultrasonic cleaner in petroleum ether and, later, deionised water.

2.2 Electrochemical characterization

Electrochemical experiments were conducted in a standard three-electrode cell with 0.25 cm^2 of exposed area in the working electrode, having a platinum mesh as a counter electrode and a saturated calomel electrode (SCE) as reference. The electrolyte used to simulate the physiological medium was naturally aerated Ringer's solution (8.61 g l^{-1} NaCl + 0.30 g l^{-1} KCl + 0.49 g L^{-1} $CaCl_2$). The exposed surfaces of the working electrodes were prepared by sequential grinding with silicon carbide paper up to 2,000 grit size followed by mechanical polishing to 1 μm with diamond paste. All experiments were carried out at 37°C, and the alloys were studied on as-cast conditions. Open circuit potential measurements, E_{OC}, for Grade 2 Ti, Zr-2.5Nb and Zr-1.5Nb-1Ta alloys were carried out on freshly polished samples, in naturally aerated aqueous electrolyte without stirring, immediately after polishing. The E_{OC} was continuously monitored during 360 h exposure. EIS measurements were carried out at open circuit potential using an EG&G PAR system Model 2263 driven by a computer. The impedance spectra were acquired in the frequency range from 100 kHz to 10 mHz at seven points per decade. The amplitude of the sinusoidal perturbation signal was 10 mV. EIS plots were obtained as a function of exposure time to the aggressive environment. EIS tests were carried out in triplicate to evaluate results reproducibility.

2.3 Biocompatibility analysis

2.3.1 Cell cultures

Human osteosarcoma cell line (Saos-2) [31] and human primary bone marrow stromal cells (BMSC; Lonza Inc., Walkersville, MD, USA) were used. All cells were expanded in plastic dishes using standard Coon's modified Ham's F12 medium (Biochrom AG, Berlin, Germany) supplemented with 10% fetal calf serum (FCS, GIBCO-Invitrogen, Milano, Italy) in a humidified atmosphere with 5% CO_2 at 37°C. BMSC were supplemented with 10 ng/mL of Fibroblast Growth Factor 2 (FGF-2; Peprotech EC, London, UK), grown and used within passage 4. Cells were cultured, trypsinized, collected and counted with standard procedures [32]. Cells were resuspended in complete medium and seeded onto the different supports (plastic, CN; Grade 2 titanium, Ti; Zr-2.5Nb alloy, BIN; Zr-1.5Nb-1Ta alloy, TER) to a final concentration of 2×10^5 cells/ml. Discs of each metal alloy under testing (approx. 4 mm in diameter) were heat-sterilized and placed in 1% agarose coated 24-multiwell plates, to avoid cell attachment onto the well surfaces. Aliquots corresponding to 10,000 cells were deposited onto the surfaces of each material under testing, plastic included, and let adhere for 4 h at 37°; then the supports were washed with PBS and supplemented with fresh medium for further testing. Cultures on plastic were performed in parallel as controls. To all cultures complete medium was changed twice a week. Two different cultures of Saos-2 and two different pools of BMSC, (each derived from two separate donors) were used for the experiments. Osteogenic induction was performed on subconfluent BMSC cultures, either on plastic or on titanium alloys, by the exposure to a differentiation factors-enriched medium (F12 medium supplemented with 10% FCS, 2.5×10^{-4}M ascorbic acid, 1.0×10^{-2}M β-glycerophosphate; 1.0×10^{-7}M dexamethasone) for 2 weeks, as elsewhere described [33]. Non induced control cultures (CN–) were maintained in standard medium.

2.3.2 Growth kinetics

DNA analysis was performed essentially as described by Zerega et al. [34]. After extensive washings, cells were lysed in situ with a SDS solution (0.01% in PBS). The lysates (100 μl) were normalized with Tris/HCl pH 7.8 and EDTA, pH 7.3 (final concentrations in samples of 200 and 50 μM, respectively), supplemented with proteinase K (final concentration 0.2 μg/ml) and heated overnight at 50°C in a thermobath. Samples were then centrifuged for 5 min at 400×*g* and supernatants collected in a clean tube. Aliquots were incubated with a Hoechst 33258 Stain Solution (Sigma-Aldrich srl, Milano, Italy; 0.5 μg/ml) for 5 min at RT. Readings were performed on a SPECTRAmax-Gemini spectrophotofluorimeter (Molecular Devices Inc., CA, USA; ex: 358 nm; Em: 458; cut-off: 455 nm). Triplicate of each sample, for each alloy and each time-point were assessed.

2.3.3 mRNA quantitative real time PCR reactions

Messenger mRNA extraction was performed using the PerfectPure RNA Cultured Cell Kit (5′-Prime GmbH, Hamburg, Germany), according to the manufacturer's instructions. Reverse transcription was performed using the SuperScript™ III first-strand synthesis system (Invitrogen, Milano, Italy). The primer sets for the genes of interest were purposely designed, custom-synthesized and purchased from TibMolBiolsrl (Genova, Italy); sequences are summarized in Table 1. Syber green real-time RT-PCR protocols were performed using the RealMasterMix SYBR ROX 2.5X (5′-Prime). The same reaction conditions were applied to assess each gene of interest, to avoid experimental bias; first we performed a denaturing step at 95°C for 3 min, followed by 30 cycling steps at 94° for 30 s, 60°C for 30 s and 72°C for 30 s. Specificity of the reaction was assayed by thermal denaturation. Real time reactions were performed in a Eppendorf Mastercycler Realplex^2 apparatus (Eppendorf Italia srl, Milano, Italy). Relative transcript levels in each target sample were referred to standard curves of serial cDNA dilutions and normalized to the corresponding target quantity of the GAPDH calibrator gene.

3 Results and discussion

3.1 Microstructural characterization

SEM characterization of Zr-2.5Nb and Zr-1.5Nb-1Ta alloys showed homogeneous morphologies, with no local discontinuities. Moreover, electron probe microanalysis confirmed calculated overall composition, detecting no composition inhomogeneities.

Both the alloys showed a single-phase morphology, crystallizing in *hP2* Mg-type (α-Zr) structure, revealed by XRD data, corresponding to equilibrium (α-Zr) solid solution.

Morphology and phases composition of these alloys are in agreement with the corresponding phase diagram [35, 36]. Lattice parameters, here not reported, resulted in agreement with literature [36].

3.2 Electrochemical characterization

The open circuit potentials, E_{OC}, variation with exposure time of Grade 2 Ti, Zr-2.5Nb and Zr-1.5Nb-1Ta alloys in Ringer's solution at 37°C, for a period of 360 h are shown in Fig. 1. Almost immediately after exposure, the potential of the Grade 2 Ti is approximately −345 mV(SCE), and it stabilizes at −170 mV(SCE) after 24 h exposure. The potential then increases slowly and reaches approximately −155 mV(SCE) after 360 h.

For the Zr-2.5Nb alloy, the initial open circuit potential is around −245 mV(SCE), and it rapidly increases to more noble potentials, reaching values around −110 mV(SCE) after 24 h exposure. The potential is quite stable after 24 h, and approximately −100 mV(SCE) after 360 h.

The variation of E_{OC} with time for the Zr-1.5Nb-1Ta alloy is similar to that for the Zr-2.5Nb alloy. The initial potential is approximately −155 mV(SCE), then it increases rapidly and after 24 h exposure it remains stable at approximately −50 mV(SCE). After 360 h the E_{OC} for this alloy is −45 mV(SCE).

In all cases the drifting towards less negative potentials is indicative that the metal surfaces are being spontaneously passivated in Ringer's solution due to the formation of an oxide film. By comparing the results reported in Fig. 1, it can be observed that the Zr-1.5Nb-1Ta alloy presents the least negative E_{OC} values, while the Grade 2 Ti exhibits the most negative E_{OC} values. These behaviours indicate that the tendency for the formation of a spontaneous oxide is greater for the Zr-1.5Nb-1Ta alloy and that this oxide has better corrosion protection characteristics than the ones formed on Grade 2 Ti or on the Zr-2.5Nb alloy in Ringer's solution.

Figure 2 reports the impedance spectra, presented as Bode plots, obtained at E_{OC} for Grade 2 Ti, Zr-2.5Nb and Zr-

Table 1 Forward and reverse primer couples for the assessed genes

Gene	Forward primer	Reverse primer
GAPDH	ACCCACTCCTCCACCTTTgA	CTgTTgCTgTAgCCAAATTCgT
BSP	gAAgAAgAgACTTCAAATg	TATCCCCagCCTTCTTgggA
RUNX2	CTTCATTCgCCTCACAAACA	TTgATgCCATAgTCCCTCCT
OP	TggCTAAACCCTgACCCATCT	gCTTTCgTTggACTTACTTggAA
OC	CgCCgCCggCAgCTACCA	TCAgAgATTTCCTCCCggATA
Col1	TTgCTCCCCAgCTgTCTTAT	TCCCCATCATCTCCATTCTT
CD146	CAgCAAgCAgAACCCCAgCA	ggACgTCAgACACATAgTTCA

GAPDH glyceraldehyde-3-phosphate dehydrogenase; *BSP* bone sialoprotein; *RUNX-2* Core binding factor a-1 (Cbf-a1); *OP* osteopontin; *OC* osteocalcin; *Col1* type I collagen; *CD146* MUC-18

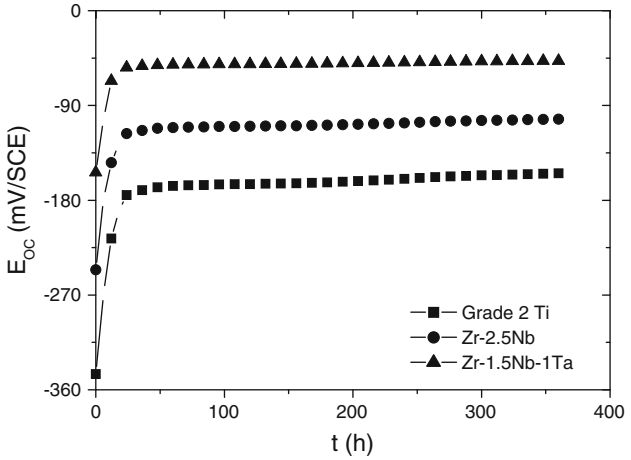

Fig. 1 Corrosion potential versus time profile for Grade 2 Ti, Zr-2.5Nb and Zr-1.5Nb-1Ta alloys after different exposure times to Ringer's physiological solution

1.5Nb-1Ta alloys at different exposure times to Ringer's solution. In all cases the impedance values increase with exposure time to the aggressive environment. The phase angle, θ, is a sensitive parameter used to indicate the presence of additional time constants in the impedance spectra at the highest and lowest frequencies. The use of the log |Z| versus log f format enables an equal representation of all experimental over the entire frequency domain [37].

The Bode plots in Fig. 2 in the frequency range between 100 kHz and 10 mHz present only 1 time constant and a near capacitive response with a phase angle close to 90° and linear variation between log |Z| and log f, in a wide range of frequencies, with a slope close to 1.

High impedance values (in the order of 10^6 Ω cm^2) were obtained for medium to low frequencies in all the samples, suggesting high corrosion resistance in the aggressive environment considered, and are indicative of a single, thin passive oxide film present at the surface of the specimens [38, 39] since the beginning of exposure.

A satisfactory fit (see Fig. 3 for the Zr-1.5Nb-1Ta alloy) of all the data could be obtained using a simple $R_s(QR_p)$ circuit (Fig. 4), where R_s and R_p are the solution and the parallel (film) resistances, respectively, and Q is a constant phase element (CPE), which takes account the capacitive behaviour of the film. This equivalent circuit has been generally used to fit oxides grown on Ti and Zr alloys under different situations [40–43]. The impedance, Z_{CPE}, of *CPE* is described by the expression [44]:

$$Z_{CPE} = [Q(j\omega)^n]^{-1}$$

with $-1 \leq n \leq 1$ and $j = \sqrt{-1}$, while Q is a frequency independent constant, being defined as pure capacitance for $n = 1$, resistance for $n = 0$, inductance for $n = -1$. Diffusion processes are characterized by the value of $n = 0.5$.

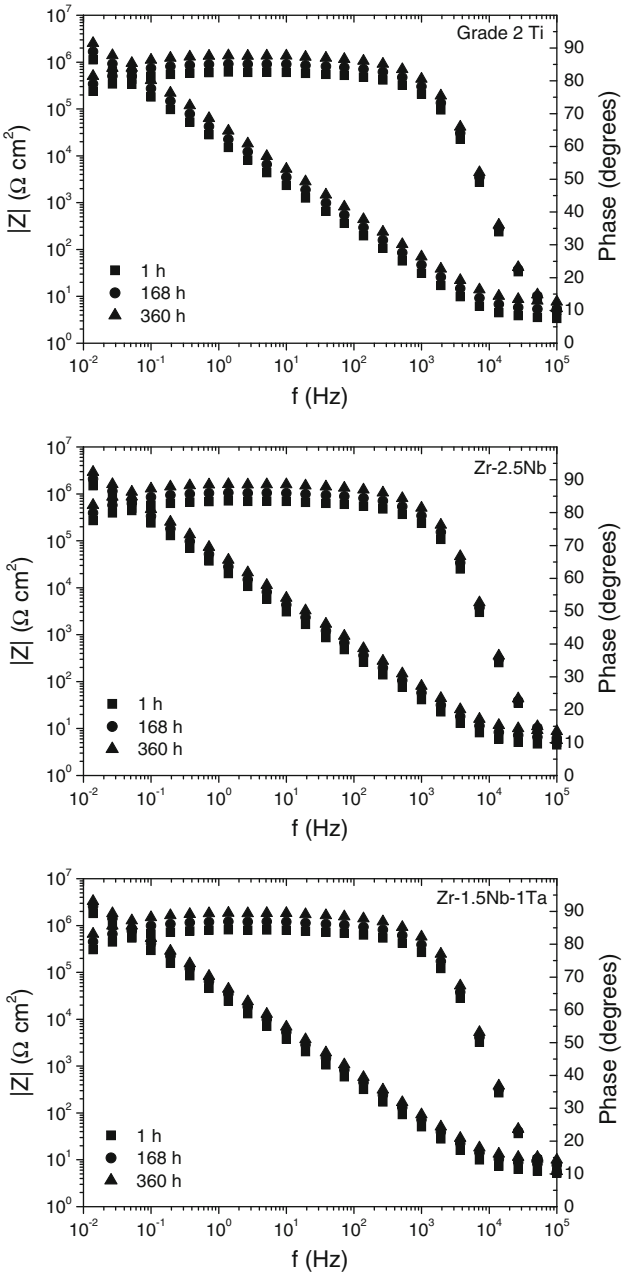

Fig. 2 Bode diagrams for Grade 2 Ti, Zr-2.5Nb and Zr-1.5Nb-1Ta alloys after different exposure times to Ringer's physiological solution

According to the fitting results, the n values are near 1 indicating that Q presents an almost pure capacitive behaviour.

The variation of the film resistance, R_p, and the capacitance, Q, with time in Ringer's solution is illustrated in Fig. 5. It can be seen in Fig. 5a that the capacitance decreases, in all cases, with increasing exposure time to the aggressive environment, indicating that the oxide film stability increases with increasing exposure time to Ringer's solution. The film resistance, R_p (Fig. 5b) has the same order of magnitude, 10^6 Ω cm^{-2}, obtained by other authors

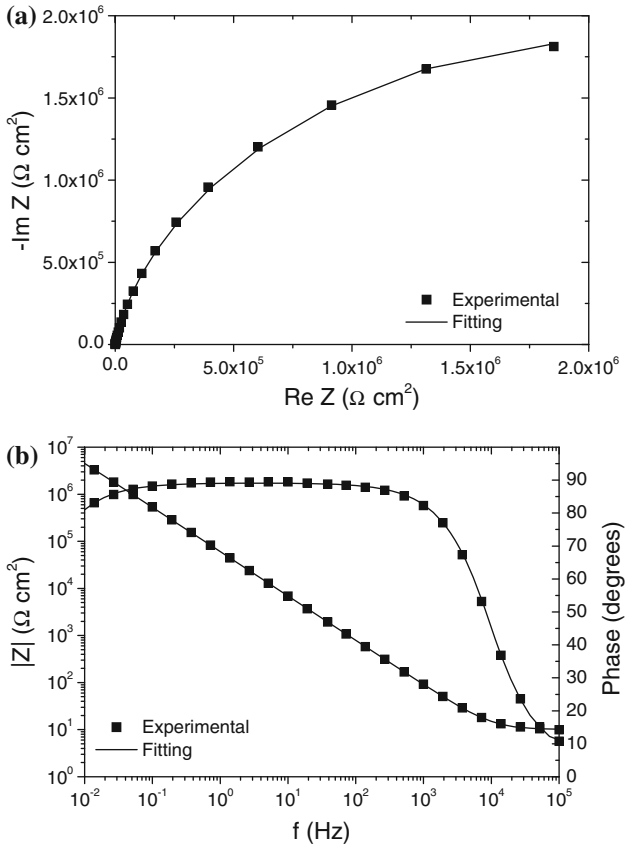

Fig. 3 **a** Nyquist and **b** Bode diagrams for Zr-1.5Nb-1Ta alloy after 360 h exposure to Ringer's physiological solution and its fitting with the equivalent circuit, $R_s(R_pQ)$, from Fig. 4

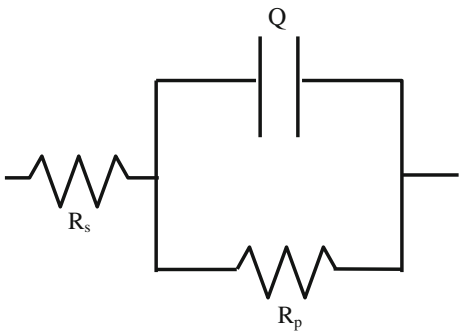

Fig. 4 Equivalent circuit, $R_s(QR_p)$, used to fit the experimental impedance data

studding different Ti alloys [39–41], and it increases with exposure time, demonstrating that the spontaneously formed oxide film on Grade 2 Ti, Zr-2.5Nb and Zr-1.5Nb-1Ta alloys becomes more resistive with exposure time. Finally, the lowest Q and highest R_p values for Zr-1.5Nb-1Ta show that this alloy has better corrosion resistance and higher stability than the other metals studied at 360 h exposure to Ringer's solution, which agrees with and confirms the results obtained from the open circuit potential measurements (Fig. 1).

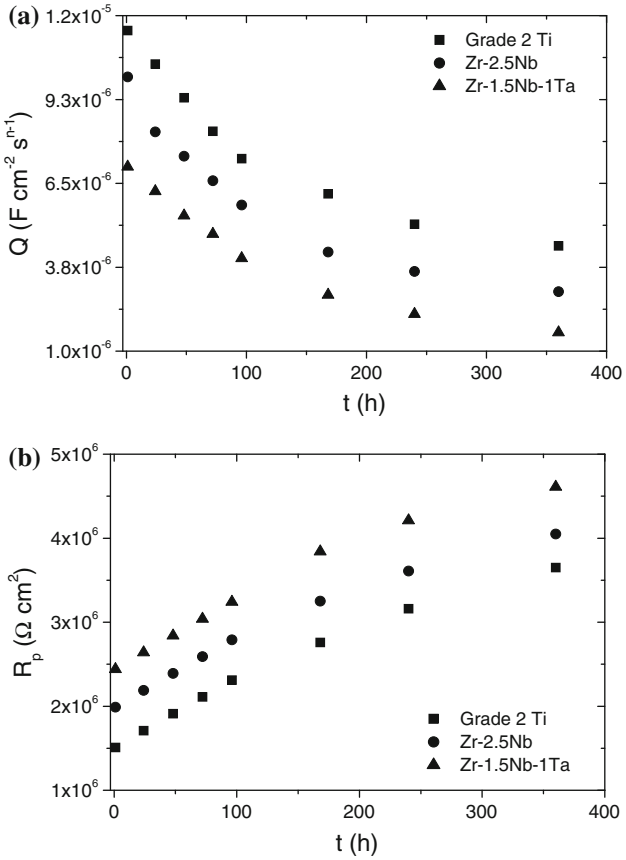

Fig. 5 **a** Capacitance, Q, and **b** polarization resistance, R_p, for Grade 2 Ti, Zr-2.5Nb and Zr-1.5Nb-1Ta alloys after different exposure times to Ringer's physiological solution

3.3 Biocompatibility

DNA content in Saos-2 and BMSC cultures was assayed to evaluate the proliferation of both cell types onto the experimental (Ti, BIN, TER) and reference (Plastic) surfaces. Data was expressed as the OD values of the nucleic acid content in each sample, normalized to the average value of the samples from control cultures, performed on plastic, at time zero. Saos-2 cells grew on all surfaces essentially at the same rate (Fig. 6a), displaying no contact inhibition and a duplication rate of about 2 days, reaching an average 14,8-fold increase in DNA content within the experimental timings. On the other hand, BMSC proliferated to a lower rate on any of the assessed surfaces, plastic included, with a duplication time of about 3–4 days (Fig. 6b). Cell growth on any of the tested metal surfaces displayed slightly poorer performances than on plastic, particularly during the initial days of culturing (Fig. 6b, compare lines Ti, BIN and TER with CN). By day 7, however, there were no substantial differences among the tested alloys, pure titanium and the controls run on plastic. As expected in tumor-derived lines, Saos-2 displayed a fast

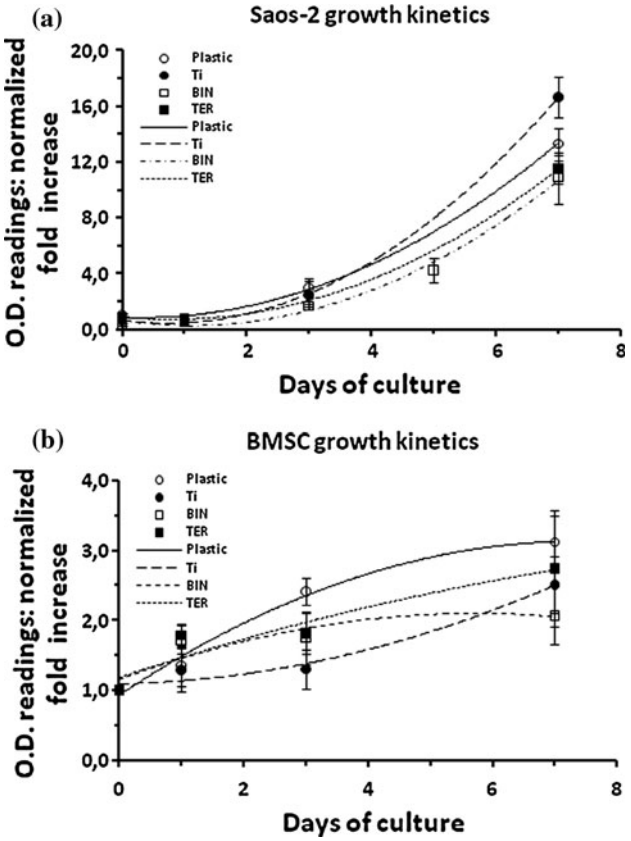

Fig. 6 **a** Growth kinetics of Saos-2 cells. Data is normalized to the OD readings of control samples cultured on plastic (Plastic). Curves refers to growth kinetics on the different surfaces as detailed in the legend; Ti: Grade 2 Ti, BIN: Zr-2.5Nb and TER: Zr-1.5Nb-1Ta alloys. Experimental data points are the mean ± SD of three determinations in two independent experiments. **b** Growth kinetics of BMSC cells. Data is normalized to the OD readings of control samples cultured on plastic (Plastic). Curves as for **a**. Experimental data points are the mean ± SD of three determinations in two independent experiments

growth rate: they are unleashed from contact inhibition and their relatively early stage of differentiation accounts even more for a reduced dependency from matrix deposition and microenvironment recognition [45]. On the contrary BMSC encompass the progenitors of mesenchymal tissues deputed to bone repair and primarily involved in the osteointegration processes of prosthetic surfaces [46–48]. For BMSC, crosstalk with the microenvironment and attachment surfaces may be fundamental to address the cells to specific differentiation fates. Therefore, their dependency upon substrate recognition and matrix deposition may explain a reduced proliferation and may be responsible of an initial reduced cell attachment to the alloy surfaces [32]. Alternatively, the growth of only limited selected cell subtypes may account for the same outcomes, once attachment requirements are satisfied. Given the envisioned use of the experimental alloys for prosthetic devices, we verified that the differentiation potential of BMSC cells was not altered upon culturing on the experimental surfaces. In vitro differentiation was induced by stimulating confluent BMSC cultures with an osteogenic factor-enriched medium for 14 days, as previously reported [33]. Induction proved successful, as indicated by the increased expression of several genes involved in the osteogenic differentiation, in stimulated versus unstimulated control cultures (Fig. 7, confront CN(–) vs. CN values). Expression levels of classical osteogenic markers, such as and BSP [49] and RUNX2 [50], were clearly elicited upon addition of the enriched medium in any of the tested surfaces, ranging between 30–90-fold, and 5–10-fold of the un-stimulated control level, respectively. Maximal expression was detected in cells grown on plastic, progressively diminishing in Ti, BIN and TER alloys, although still relevant if confronted with unstimulated cells (Fig. 7). BSP displays the biophysical and chemical characteristics of a nucleator and its expression is known to coincide with mineralization in bone and cementum [51]. The contemporary upregulation of RUNX2 keeps also in line with previous reports, since this transcription factor known to directly control BSP expression [52]. Moreover, both RUNX2 and osteocalcin are pre-requisites, in BMSC, for matrix deposition and mineralization [50]. It should be noted, however, that after the upregulatory burst RUNX2 and osteocalcin are known to reduce their expression to control levels even under simultaneous exposure to osteogenic stimuli [53, 54] as well as during the late events of bone repair and remodeling [55]. On our experimental surfaces osteopontin (OP) was upregulated on pure titanium (Fig. 7, 2.94 ± 0.10; mean ± SD values of normalized expression level) with respect to unstimulated or osteogenically stimulated control cells; values returned to control levels in cells cultured onto BIN or TER alloys. The mRNA level for osteopontin was already demonstrated to increase upon osteoblast-like cell seeding onto P- and/or Sr-enriched titanium surfaces [56] whereas it did not show any difference between dual acid-etched- or machined-etched titanium surfaces [57]. Recently $OP^{-/-}$ mice were shown to display an impaired NK cell maturation in the bone microenvironment [58]; however, although significant, the reduced expression of OP in the osteogenically induced BMSC seeded onto the BIN and TER alloys still complies with expression values derived from osteogenically-induced cells grown on plastic. Interestingly, in vitro extracellular matrix enriched-titanium scaffolds were demonstrated to enhance the mineralized matrix deposition of BMSC by sustaining the expression of specific gene subsets, among which OP itself [59]. In our settings the pure titanium surface seems to drive the strongest expression of matrix components (namely BSP and RUNX2), possibly self-contributing to a more elevated OP expression. Conversely, among the tested genes, transcript levels for

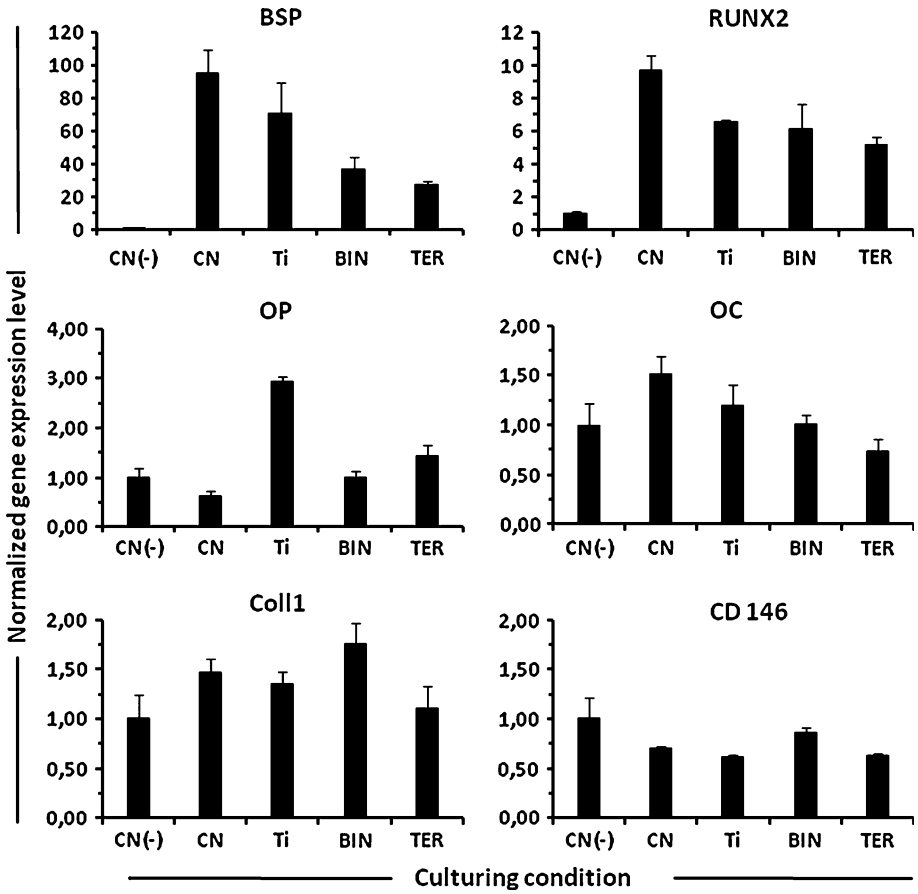

Fig. 7 Expression levels of osteogenic markers in BMSC cultured on different surfaces. Levels of mRNA for bone sialoprotein (BSP), core binding factor 2 (RUNX2), osteopontin (OP), osteocalcin (OC), type I collagen (Coll 1) and CD 146 are depicted for each surface: *CN* plastic; *Ti* Grade 2 Ti, *BIN* Zr-2.5Nb and *TER* Zr-1.5Nb-1Ta alloys; normalization was performed with respect to the level of each assessed gene as in BMSC cultured on plastic before the osteogenic induction (CN–); Histograms depict normalized gene expression values ± SD of three determinations as assayed by real-time RT-PCR

osteocalcin (OC), type I collagen (Coll 1) or CD146 did not display significant variations when cells were seeded onto the different surfaces under testing.

As a whole our expression data, then, may indicate that the effects of the osteogenic induction are slightly less evident in the BIN and TER alloys, possibly due to a different sensitivity to oxidation of the available surfaces, initial cell attachment and matrix deposition. Nevertheless, none of the tested surfaces is hindering the differentiation properties of the BMSC or the biochemical stimuli of the environment. In this respect, an essentially unaltered expression level among the different alloys for CD146 mRNA, a recognized marker of cells capable of establishing the hematopoietic microenvironment in human bone marrow [60], indicates that the assessed surfaces had not undertaken a selective effects on the seeded bone progenitors, and may be thus foreseen for prosthetic applications in the light of their additional properties.

4 Conclusions

The in vitro corrosion behavior and biocompatibility of two Zr alloys, Zr-2.5Nb, employed for the manufacture of CANDU reactor pressure tubes, and Zr-1.5Nb-1Ta (at%), for use as implant materials have been assessed and compared with those of Grade 2 Ti, which is known to be a highly compatible metallic biomaterial. The in vitro corrosion resistance was investigated by open circuit potential and EIS measurements, as a function of exposure time to an artificial physiological solution. The results can be summarized as follows:

1. Open circuit potential, E_{OC}, values indicated that both the Zr alloys and Grade 2 Ti undergo spontaneous passivation due to spontaneously formed oxide film passivating the metallic surface, in the aggressive environment. Zr-1.5Nb-1Ta alloy presented the highest E_{OC} values, while the Grade 2 Ti exhibited the lowest E_{OC} values, indicating that the tendency for the formation of a spontaneous oxide is greater for the Zr-1.5Nb-1Ta alloy and that this oxide has better corrosion protection characteristics than the ones formed on Grade 2 Ti or on the Zr-2.5Nb alloy.
2. High impedance values were obtained for all samples, and its increase with exposure time to the aggressive solution indicated an improvement in corrosion resistance of the spontaneous oxide film. The fit obtained suggests a single passive film presents on the metals surface, with resistance improving with exposure time.

The Zr-1.5Nb-1Ta alloy presented the highest R_p values, showing that the alloy had better corrosion resistance and higher stability than the other metals studied.

3. Biocompatibility tests showed that Saos-2 cells grow rapidly, independently of the surface, due to reduced dependency from matrix deposition and microenvironment recognition. BMSC instead display a reduced proliferation, possibly caused by a reduced crosstalk with the metal surface microenvironment. However, once the substrate has been colonized, BMSC seem to respond properly to osteoinduction stimuli, thus supporting a substantial equivalence in the biocompatibility among the Zr alloys and Grade 2 titanium.

The high in vitro corrosion resistance together with a satisfactory biocompatibility make the Zr-2.5Nb and Zr-1.5Nb-1Ta crystalline alloys promising biomaterials for surgical implants.

References

1. Lohrengel MM. Formation of ionic space charge layers in oxide films on valve metals. Electrochim Acta. 1994;39:1265.
2. Malik F. A study of passive films on valve metals. Thin Solid Films. 1991;206:345.
3. Bockris JOM. Modern aspect of electrochemistry, vol. 14. New York: Plenum Press; 1982.
4. Badawy WA, Felske A, Plieth WJ. Electrochemical, photoelectrochemical behaviour of passivated Ti, Nb electrodes in nitric acid solutions. Electrochim Acta. 1989;34:1711.
5. Biaggio SR, Rocha-Filho RC, Vilche JR, Varela FE, Gassa LM. A study of thin anodic WO_3 films by electrochemical impedance spectroscopy. Electrochim Acta. 1997;42:1751.
6. Marino CEB, Oliveira EM, Rocha-Filho RC, Biaggio SR. On the stability of thin-anodic-oxide films of titanium in acid phosphoric media. Corros Sci. 2001;43:1465.
7. Salot R, Lefevbre-Joud F, Baroux B. Electrochemical behavior of thin anodic oxide films on Zircaloy-4. J Electrochem Soc. 1996;143:3902.
8. Hammad AM, El-Mashri SM, Nasr MA. Mechanical properties of the Zr-1% Nb alloy at elevated temperatures. J Nuclear Mater. 1992;186:166.
9. Oliveira NTC, Biaggio SR, Rocha-Filho RC, Bocchi N. Studies on the stability of anodic oxides on zirconium biocompatible alloys. J Braz Chem Soc. 2002;13:463.
10. Pourbaix M. Electrochemical corrosion of metallic biomaterials. Biomaterials. 1984;5:122.
11. Biehl V, Breme J. Metallic biomaterials. Mat-wiss u Werkstofftech. 2001;32:137.
12. Niinomi M, Kuroda D, Fukunaga K, Morinaga M, Kato Y, Yashiro T, Suzuki A. Corrosion wear fracture of new β type biomedical titanium alloys. Mater Sci Eng A. 1999;263:193.
13. Okazaki Y, Rao S, Tateishi T, Ito Y. Cytocompatibility of various metals and development of new titanium alloys for medical implants. Mater Sci Eng A. 1998;243:250.
14. Bjursten LM, Emanuelsson L, Ericson LE, Thomsen P, Lausmaa J, Mattson L, Rolander U, Kasemo B. Method for ultrastructural studies of the intact tissue-metal interface. Biomaterials. 1990;11:596.
15. Thompsen P, Larsson C, Ericson LE, Sennerby L, Lausmaa J, Kasemo B. Structure of the interface between rabbit cortical bone and implants of gold, zirconium and titanium. J Mater Sci: Mater Med. 1997;8:653.
16. Sherepo KM, Red'ko IA. Use of zirconium for implants in traumatology and orthopedics. Med Tekh. 2004;2:22.
17. Cabrini RL, Guglielmotti MB, Almagro JC. Histomorphometry of initial bone healing around zirconium implants in rats. Implant Dent. 1993;2:264.
18. Guglielmotti MB, Cabrini RL, Guerrero C. Chronodynamic evaluation of the stages of osseointegration in zirconium laminar implants. Acta Odontol Latinoam. 1997;10:11.
19. Guglielmotti MB, Cabrini RL, Renou S. A histomorphometric study of tissue interface by laminar test in rats. Int J Oral Maxillofac Implants. 1999;14:565.
20. Kulokaov OB, Doktorov AA, D'iakova SV, Denisov-Nikol'skii IuI, Grotz KA. Experimental study of osseointegration of zirconium and titanium dental implants. Morfologiia. 2005;127:52.
21. Cox B. Advances in corrosion science and technology, vol. 5. New York: Plenum Press; 1976.
22. Yun YH, Turitto VT, Daigle KP, Kovacs P, Davidson JA, Slack SM. Initial, hemocompatibility studies of titanium and zirconium alloys: Prekallikrein activation, fibrinogen adsorption, and their correlation with surface electrochemical properties. J Biomed Mater Res. 1996;32:77.
23. Helsen JA, Breme J. Metals as biomaterials. Chichester, England: Wiley; 1998.
24. Matsuno H, Yokoyama A, Watary F, Uo M, Kawasaki T. Biocompatibility and osteogenesis of refractory metal implants, titanium, hafnium, niobium, tantalum and rhenium. Biomaterials. 2001;22:1253.
25. Gerardi S. ASTM Handbook, vol. 2. Metals Park: ASM International; 1993.
26. Eisenbarth E, Velten D, Müller M, Thull R, Breme J. Biocompatibility of β-stabilizing elements of titanium alloys. Biomaterials. 2004;25:5705.
27. Branzoi IV, Iordoc M, Codescu M. Electrochemical studies on the stability and corrosion resistance of new zirconium-based alloys for biomedical applications. Surf Interface Anal. 2008;40:167.
28. Yto A, Okazaki Y, Tateishi T, Ito Y. Mechanical properties of the binary titanium-zirconium alloys and their potential for biomedical materials. J Biomed Mater Res. 1995;29:943.
29. Khan MA, Williams RL, Williams DF. In vitro corrosion and wear of titanium alloys in the biological environment. Biomaterials. 1996;17:2117.
30. Rosalbino F, Macciò D, Saccone A, Angelini E, Delfino S. Effect of Nb alloying additions on the characteristics of anodic oxide films on zirconium and their stability in NaOH solution. J Solid State Electrochem. 2010;14:1451.
31. Rodan SB, Imai Y, Thiede MA, Wesolowski G, Thompson D, Bar-Shavit Z, Shull S, Mann K, Rodan GA. Characterization of a human osteosarcoma cell line (Saos-2) with osteoblastic properties. Cancer Res. 1987;47:4961.
32. Giannoni P, Muraglia A, Giordano C, Narcisi R, Cancedda R, Quarto R, Chiesa R. Osteogenic differentiation of human mesenchymal stromal cells on surface-modified titanium alloys for orthopedic and dental implants. Int J Artif Organs. 2009;32:811.
33. Muraglia A, Cancedda R, Quarto R. Clonal mesenchymal progenitors from human bone marrow differentiate in vitro according to a hierarchical model. J Cell Sci. 2000;113:1161.
34. Zerega B, Cermelli S, Bianco P, Cancedda R, Cancedda FD. Parathyroid hormone [PTH(1–34)] and parathyroid hormone-related protein [PTHrP(1–34)] promote reversion of hypertrophic chondrocytes to a prehypertrophic proliferating phenotype and prevent terminal differentiation of osteoblast-like cells. J Bone Miner Res. 1999;14(8):1281.

35. Abriata JP, Bolcich JC. The Nb–Zr (Niobium–Zirconium) system. Bull Alloy Phase Diag. 1982;3(1):34.
36. Villars P, Prince A, Okamoto H. Handbook of ternary alloy phase diagrams. Metals Park, Ohio: ASM International; 1995.
37. Metikos-Hukovic M, Kwokal A, Piljac J. The influence of niobium and vanadium on passivity of titanium-based implants in physiological solution. Biomaterials. 2003;24:3765.
38. Oliveira NTC, Aleixo G, Caram R, Guastaldi AC. Development of Ti–Mo alloys for biomedical applications: microstructure and electrochemical characterization. J Mater Sci Eng A. 2007; 452–453:727.
39. Temiselvi S, Raman V, Rajendran N. Corrosion behaviour of Ti-6Al-7Nb and Ti-6Al-4 V ELI alloys in the simulated body fluid solution by electrochemical impedance spectroscopy. Electrochim Acta. 2006;52:839.
40. Gonzalez JEG, Mirza-Rosca JC. Study of the corrosion behaviour of titanium and some of its alloys for biomedical and dental implant applications. J Electroanal Chem. 1999;471:109.
41. Shukla AK, Balasubramaniam R. Effect of surface treatment on electrochemical behavior of CP Ti, Ti-6Al-4 V and Ti-13Nb-13Zr alloys in simulated human body fluid. Corros Sci. 2006;48: 1696.
42. Oliveira NTC, Biaggio SR, Piazza S, Sunseri C, Di Quarto F. Photo-electrochemical and impedance investigation of passive layers grown anodically on titanium alloys. Electrochim Acta. 2004;49:4563.
43. Martins DQ, Osório WR, Souza MEP, Caram R, Garcia A. Effect of Zr content on microstructure and corrosion resistance of Ti-30Nb-Zr casting alloys for biomedical applications. Electrochim Acta. 2008;53:2809.
44. Macdonald JR. Impedance spectroscopy. New York: Wiley; 1987.
45. Mackie EJ, Ramsey SJ. Modulation of osteoblast behaviour by tenascin. Cell Sci. 1996;106:1597.
46. Haynesworth SE, Goshima J, Goldberg VM, Caplan AI. Characterization of cells with osteogenic potential from human marrow. Bone. 1992;13(1):81.
47. Braccini A, Wendt D, Jaquiery C, Jakob M, Heberer M, Kenins L, Wodnar-Filpowicz A, Quarto R, Martin I. Three-dimensional perfusion culture of human bone marrow cells and generation of osteoinductive grafts. Stem Cells. 2005;23:1066.
48. Giannoni P, Mastrogiacomo M, Alini M, Pearce SG, Corsi A, Santolini F, Muraglia A, Bianco P, Cancedda R. Regeneration of large bone defects in sheep using bone marrow stromal cells. J Tissue Eng Regen Med. 2008;2:253.
49. Zreiqat H, Howlett CR. Titanium substrata composition influences osteoblastic phenotype: In vitro study. J Biomed Mater Res. 1999;47:360.
50. Marom R, Shur I, Solomon R, Benayahu D. Characterization of adhesion and differentiation markers of osteogenic marrow stromal cells. J Cell Physiol. 2005;202:41.
51. Ganss B, Kim RH, Sodek J. Bone sialoprotein. Crit Rev Oral Biol Med. 1999;10:79.
52. Roca H, Phimphilai M, Gopalakrishnan R, Xiao G, Franceschi RT. Cooperative interactions between RUNX2 and homeodomain protein-binding sites are critical for the osteoblast-specific expression of the bone sialoprotein gene. J Biol Chem. 2005;280:30845.
53. Carvalho RS, Bumann A, Schaffer JL, Gerstenfeld LC. Predominant integrin ligands expressed by osteoblasts show preferential regulation in response to both cell adhesion and mechanical perturbation. J Cell Biochem. 2002;84:497.
54. Lamour V, Detry C, Sanchez C, Henrotin Y, Castronovo V, Bellahcene A. Runx2- and histone deacetylase 3-mediated repression is relieved in differentiating human osteoblast cells to allow high bone sialoprotein expression. J Biol Chem. 2007;282: 36240.
55. Behonick DJ, Xing Z, Lieu S, Buckley JM, Lotz JC, Marcucio RS, Werb Z, Miclau T, Colnot C. Role of matrix metalloproteinase 13 in both endochondral and intramembranous ossification during skeletal regeneration. PLoS ONE. 2007;2:e1150.
56. Park JW, Kim YJ, Jang JH. Enhanced osteoblast response to hydrophilic strontium and/or phosphate ions-incorporated titanium oxide surfaces. Clin Oral Implants Res. 2010;21(4):398.
57. Balloni S, Calvi EM, Damiani F, Bistoni G, Calvitti M, Locci P, Becchetti E, Marinucci L. Effects of titanium surface roughness on mesenchymal stem cell commitment and differentiation signaling. Int J Oral Maxillofac Implants. 2009;24(4):627.
58. Chung JW, Kim MS, Piao ZH, Jeong M, Yoon SR, Shin N, Kim SY, Hwang ES, Yang Y, Lee YH, Kim YS, Choi I. Osteopontin promotes the development of natural killer cells from hematopoietic stem cells. Stem Cells. 2008;26(8):2114.
59. Pham QP, Kasper FK, Scott Baggett L, Raphael RM, Jansen JA, Mikos AG. The influence of an in vitro generated bone-like extracellular matrix on osteoblastic gene expression of marrow stromal cells. Biomaterials. 2008;29(18):2729.
60. Sacchetti B, Funari A, Michienzi S, Di Cesare S, Piersanti S, Saggio I, Tagliafico E, Ferrari S, Gheron Robey P, Riminucci M, Bianco P. Self-renewing osteoprogenitors in bone marrow sinusoids can organize a hematopoietic microenvironment. Cell. 2007;131:324.